Quantum Phase Diagram of the Triangular-Lattice *XXZ* Model in a Magnetic Field

Daisuke Yamamoto,[1] Giacomo Marmorini,[1,2] and Ippei Danshita[3]
[1]*Condensed Matter Theory Laboratory, RIKEN, Saitama 351-0198, Japan*
[2]*Research and Education Center for Natural Sciences, Keio University, Kanagawa 223-8521, Japan*
[3]*Yukawa Institute for Theoretical Physics, Kyoto University, Kyoto 606-8502, Japan and Computational Condensed Matter Physics Laboratory, RIKEN, Saitama 351-0198, Japan*
(Received 3 September 2013; revised manuscript received 17 January 2014; published 26 March 2014)

The triangular lattice of $S = 1/2$ spins with XXZ anisotropy is a ubiquitous model for various frustrated systems in different contexts. We determine the quantum phase diagram of the model in the plane of the anisotropy parameter and the magnetic field by means of a large-size cluster mean-field method with a scaling scheme. We find that quantum fluctuations break up the nontrivial continuous degeneracy into two first-order phase transitions. In between the two transition boundaries, the degeneracy-lifting results in the emergence of a new coplanar phase not predicted in the classical counterpart of the model. We suggest that the quantum phase transition to the nonclassical coplanar state can be observed in triangular-lattice antiferromagnets with large easy-plane anisotropy or in the corresponding optical-lattice systems.

DOI: 10.1103/PhysRevLett.112.127203 PACS numbers: 75.10.Jm, 75.30.Kz, 75.45.+j

Introduction.—Geometric frustration arises when local interaction energies cannot be simultaneously minimized due to lattice geometry, resulting in a large ground-state degeneracy [1,2]. A variety of unconventional phenomena generated by frustration have been a fascinating and challenging subject in modern condensed matter physics. In particular, frustrated spin systems are a promising place to explore exotic states of matter such as noncolinear antiferromagnetic order [3–6], order-by-disorder selection to form magnetization plateaus [7–10], spin liquid [11,12], and lattice supersolidity [13–15]. However, established theories and numerical simulations often encounter serious difficulties including the notorious minus-sign problem [16] in dealing with frustrated systems. Thus, a reliable investigation for frustrated magnetism has been limited mainly to classical spins [17–19], the SU(2)-symmetric point of the model [3–6], or (quasi-)one-dimensional systems [20].

In this Letter, we demonstrate a possible way to overcome the problem by determining the ground-state phase diagram of frustrated quantum spins on the 2D triangular lattice over a wide range of magnetic field and exchange anisotropy. This system has also been attracting great physical interest from the experimental side since the latest developments in magnetic materials and ultracold gases have resolved technical difficulties to realize ideal 2D frustrated systems. Specifically, the compound $Ba_3CoSb_2O_9$ has been reported very recently [21–24] as the first example of ideal triangular-lattice antiferromagnet with spatially isotropic couplings and no Dzyaloshinsky-Moriya interactions. In this compound, the effective $S = 1/2$ spins of Co^{2+} ions form a regular triangular lattice unlike other known (distorted) materials such as Cs_2CuCl_4 [25], Cs_2CuBr_4 [26,27], and $\kappa-(\mathrm{BEDT}-\mathrm{TTF})_2\mathrm{Cu}_2(\mathrm{CN})_3$ [28]. The magnetization process of the single-crystal samples has shown a strong dependence on the magnetic field direction [23], which indicates the existence of the anisotropy between the in-plane (XY) and out-of-plane (Ising) exchange interactions in spin space, known as XXZ anisotropy. To properly explain the observed magnetization anomalies, it is necessary to take into account the exchange anisotropy and quantum fluctuations for arbitrary field. Furthermore, considerable advances have also been made in the direction of simulating magnetism with ultracold atomic or molecular gases in a periodic optical potential [29–32]. A frustrated XY system has indeed been realized recently [31] by dynamically inverting the sign of the hopping integral [33,34] of bosonic atoms in a triangular optical lattice [35]. In optical lattices, an Ising-type coupling can be introduced by finite-range repulsion, e.g., dipole-dipole interactions [36–38], while the XY coupling comes from the hopping. Thus, the XXZ anisotropy is widely controllable in such a system.

In connection with the ongoing experiments, we report a theoretical prediction of the quantum phase diagram of the spin-1/2 frustrated XXZ system on the triangular lattice with the following Hamiltonian [39]:

$$\hat{\mathcal{H}} = J\sum_{\langle i,j\rangle}(\hat{S}_i^x\hat{S}_j^x + \hat{S}_i^y\hat{S}_j^y) + J_z\sum_{\langle i,j\rangle}\hat{S}_i^z\hat{S}_j^z - H\sum_i\hat{S}_i^z, \quad (1)$$

where the sum $\sum_{\langle i,j\rangle}$ runs over nearest-neighbor sites. The spin-1/2 XXZ model is also an effective model describing spin-dimer compounds such as $Ba_3Mn_2O_8$, in which the isotropic couplings can induce large effective XXZ anisotropy [40], and binary mixtures of atomic gases in an optical lattice [41,42]. Despite the broad relevance and the apparent simplicity of the model (1), its quantum phase diagram in the frustrated regime ($J,\ J_z > 0$) remains

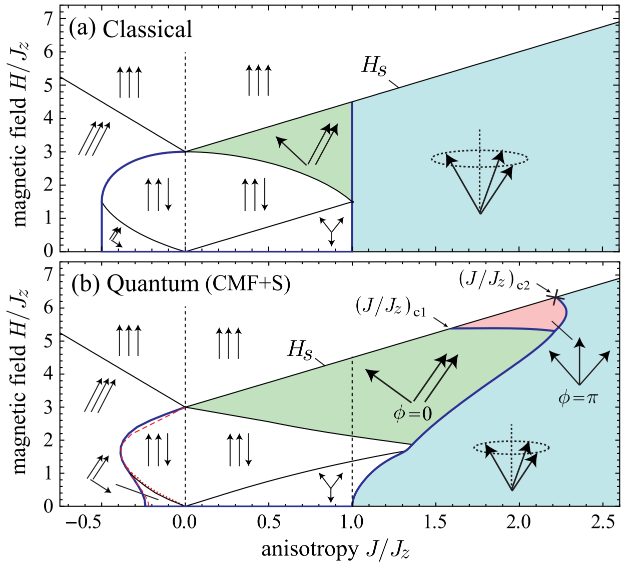

FIG. 1 (color online). Ground-state phase diagram of the spin-1/2 triangular-lattice XXZ model from (a) the classical and (b) CMF + S analyses ($J_z > 0$). The thick blue (thin black) solid curves correspond to first- (second-)order transitions. The latest QMC data [45,46] are shown by the red dashed (first-order) and dotted (second-order) curves. The symbol (×) is the value from the dilute Bose-gas expansion.

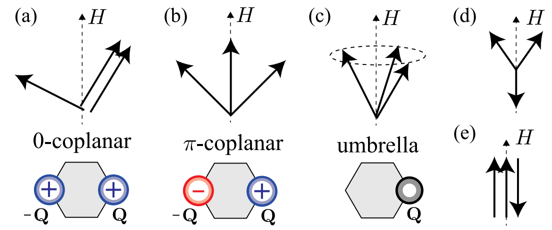

FIG. 2 (color online). Five types of spin configurations for $J/J_z > 0$. The sets of three arrows represent each spin angle on the three sublattices. The lower illustrations in (a)–(c) depict the corresponding distributions of magnon BECs at the corners of the hexagonal first Brillouin zone.

unrevealed mainly because the quantum Monte Carlo (QMC) method suffers from the minus-sign problem. Here, we avoid the usual difficulties for frustrated systems by employing the large-size cluster mean-field method combined with a scaling scheme (CMF + S) established recently in Ref. [43] and determine the complete quantum phase diagram in the whole plane of the anisotropy $-\infty < J/J_z < \infty$ and the magnetic field H/J_z for $J_z > 0$ with a high degree of accuracy (see Fig. 1). We show that quantum fluctuations drastically change the phase diagram from the classical one. In particular, we find that the nontrivial continuous degeneracy at $J/J_z = 1$ breaks up into two first-order transitions at strong fields due to the quantum effects, and a nonclassical coplanar state emerges between the two transitions. We complement the analysis with the dilute Bose gas expansion [44] near the saturation field and express the first-order transitions in terms of the magnon Bose-Einstein condensation (BEC). We also discuss a translation of the results into the bosonic language with optical-lattice experiments in mind.

Classical phase diagram.—In Fig. 1(a), we show the phase diagram obtained by the classical-spin ($S = \infty$) analysis [18,47] as reference to be compared with the quantum case. For positive easy-axis anisotropy $0 < J/J_z < 1$, one finds three different states with the three-sublattice $\sqrt{3} \times \sqrt{3}$ structure below the saturation field $H_s = 3J/2 + 3J_z$: low- and high-field coplanar states depicted in Figs. 2(d) and 2(a) and a collinear up-up-down state in Fig. 2(e). For easy-plane anisotropy $J/J_z > 1$, the so-called umbrella state in Fig. 2(c) appears. We will discuss quantum effects on the classical ground state by means of the dilute Bose-gas [44] and CMF + S [43] approaches. It is of particular interest how the ground-state degeneracy along the line of $J/J_z = 1$ [17] is lifted.

Dilute Bose-gas expansion.—The quantum magnetic structures just below H_s can be semianalytically studied using the dilute Bose-gas expansion [44,48], in which first the spin model (1) is rewritten in the hard-core boson (magnon) representation: $\hat{S}_i^z = 1/2 - \hat{a}_i^\dagger \hat{a}_i$ and $\hat{S}_i^+ = \hat{a}_i$. For the triangular lattice, the magnons $\hat{a}_{\mathbf{k}}$ in the Fourier space can condense at either or both of the two independent minima of the single-particle energy, which are located at the corners $\mathbf{k} = \pm\mathbf{Q} \equiv \pm(4\pi/3, 0)$ of the hexagonal first Brillouin zone. For $0 < H_s - H \ll H_s$, the ground-state energy per site up to fourth order in the magnon BEC order parameters $\psi_{\pm\mathbf{Q}} \equiv \langle \hat{a}_{\pm\mathbf{Q}} \rangle$ is given by

$$E_0/M = -(H_s - H)(|\psi_{\mathbf{Q}}|^2 + |\psi_{-\mathbf{Q}}|^2) + \Gamma_1(|\psi_{\mathbf{Q}}|^4 + |\psi_{-\mathbf{Q}}|^4)/2 + \Gamma_2 |\psi_{\mathbf{Q}}|^2 |\psi_{-\mathbf{Q}}|^2. \quad (2)$$

The degeneracy in the relative phase $\phi = \arg(\psi_{\mathbf{Q}}/\psi_{-\mathbf{Q}})$ between the two BECs can be lifted by the higher-order term $2\Gamma_3 |\psi_{\mathbf{Q}}|^3 |\psi_{-\mathbf{Q}}|^3 \cos 3\phi$. More details of Eq. (2) and the effective interactions Γ_1, Γ_2, and Γ_3 are presented in the Supplemental Material [49]. The ordering vectors $\pm\mathbf{Q}$ identify a three-sublattice structure consistent with the classical-spin analysis. Minimizing the ground-state energy, we obtain the following three types of solution: (i) $\Gamma_1 > \Gamma_2$ and $\Gamma_3 < 0$: $|\psi_{\mathbf{Q}}| = |\psi_{-\mathbf{Q}}| \neq 0$, $\phi = 0$; (ii) $\Gamma_1 > \Gamma_2$ and $\Gamma_3 > 0$: $|\psi_{\mathbf{Q}}| = |\psi_{-\mathbf{Q}}| \neq 0$, $\phi = \pi$; (iii) $\Gamma_1 < \Gamma_2$: $|\psi_{\mathbf{Q}}| \neq 0$ and $|\psi_{-\mathbf{Q}}| = 0$ (or vice versa).

Since the double-BEC solutions with (i) $\phi = 0$ and (ii) $\phi = \pi$ correspond to the two different coplanar states in Figs. 2(a) and 2(b) [44], we refer to them as the "0-coplanar" and "π-coplanar" states. The single-BEC solution (iii) is translated into the umbrella state in Fig. 2(c).

We calculate the coplanar-umbrella phase boundary $(J/J_z)_{c2}$ from the condition $\Gamma_1 = \Gamma_2$. In 2D systems, Γ_1 and Γ_2 vanish due to the infrared singularity in loop integrals [50]. Therefore, we introduce interlayer XXZ

couplings $J^{\perp}$, $J_z^{\perp}$ as regulators, and then take the limit of $J^{\perp}, J_z^{\perp} \to 0$ [49]. The value of $(J/J_z)_{c2}$ converges to 2.218 regardless of the sign and ratio of $J^{\perp}$ and $J_z^{\perp}$ (or, in other words, independently of the details of the regularization) [see Fig. 3(a)]. This means that the region of coplanar states is extended toward the rather large easy-plane anisotropy side due to the quantum effects [see the symbol (×) in Fig. 1(b)]. Even for $0 < H_s - H \ll H_s$, the dilute Bose-gas expansion has not been able to determine which coplanar state ($\phi = 0$ or π) emerges, because the calculation of Γ_3 is practically difficult [44]. We will see below that the CMF + S analysis unambiguously answers this long-standing question, first raised in Ref. [44].

Entire quantum phase diagram.—The complete quantum phase diagram for an arbitrary field is numerically determined by the use of the CMF + S method. We perform the exact diagonalization of a cluster system of N_C spins after the standard mean-field decoupling of the interactions between the edge and outside spins [43]. Although we treat only static mean fields unlike the (cluster) dynamical mean-field approximation [51,52], we can deal with a large-size cluster, which gives the possibility to take the infinite cluster-size limit [38,43,53]. Here, we use the series of the clusters that consist of up to $N_C = 21$ spins and self-consistently calculate $m_\mu^\alpha \equiv \langle \hat{S}_{i_\mu}^\alpha \rangle$ ($\alpha = x, y, z$) considering all possible spin structures under the three-sublattice ansatz ($\mu = A, B, C$). We find that the data for the phase boundaries obtained by the three largest clusters produce a linear extrapolation line with the scaling parameter $\lambda \equiv N_B/(N_C z/2)$ [see Fig. 3(b)], which allows us to determine the phase diagram of the frustrated spin model (1) in a quantitatively reliable way. Here, N_B is the number of bonds within the cluster and $z = 6$ is the coordination number of the triangular lattice.

The quantum phase diagram is shown in Fig. 1(b). We see that the positive (frustrated) J/J_z side is drastically changed from the classical one. The collinear up-up-down state is extended by quantum effects, which causes a plateau at one-third of the saturation magnetization in the magnetization process even for $J/J_z \geq 1$. The coplanar states are also significantly extended toward the easy-plane side for strong fields. Just below the saturation field, the scaled value of the coplanar-umbrella boundary is $(J/J_z)_{c2} = 2.220$ [see Fig. 3(b)], which is in good agreement with the value 2.218 from the dilute Bose-gas expansion. Of particular interest is the emergence of a new phase not predicted in the classical counterpart of the model for large easy-plane anisotropy $1.6 \lesssim J/J_z \lesssim 2.3$ and strong fields $H/H_s \gtrsim 0.84$ [red region in Fig. 1(b)] as a result of a novel quantum lifting mechanism (explained below). The spin structure of the nonclassical state is given by $m_A^z \neq m_B^z = m_C^z$ and $m_A^x = 0$, $m_B^x = -m_C^x$ when the ordering plane is the xz plane ($m_\mu^y = 0$). This is indeed the π-coplanar state shown in Fig. 2(b). On the other hand, $m_A^z = m_B^z \neq m_C^z$ and $m_A^x = m_B^x \neq m_C^x$ in the 0-coplanar state (green region). The $0-\pi$ transition point just below the saturation field is extrapolated to $(J/J_z)_{c1} = 1.588$, at which the sign of Γ_3 should change. The total transverse magnetization is nonvanishing in the 0-coplanar state ($2m_A^x + m_C^x \neq 0$) [39], whereas it is zero in the π-coplanar state.

The quantum phase diagram does not include any disordered phase, i.e., spin liquid. The two end points of the plateau at $J/J_z = 1$ are given by $H_{c1}/J_z = 1.345$ and $H_{c2}/J_z = 2.113$, which are consistent with the coupled cluster method [8] and the exact diagonalization with periodic boundary conditions [9]. Moreover, our result gives good agreement with the QMC data [45,46] (red curves) in the negative J/J_z side including the order of the transitions [46,54,55]. In particular, the phase transition point at $H = 0$, $(J/J_z)_0 = -0.238$, agrees with the known numerical data, $(J/J_z)_0 \approx -0.23$–-0.21 [45,46,55,56] (see the comparison table in Ref. [49]), which indicates high accuracy of the CMF + S analysis on the current problem.

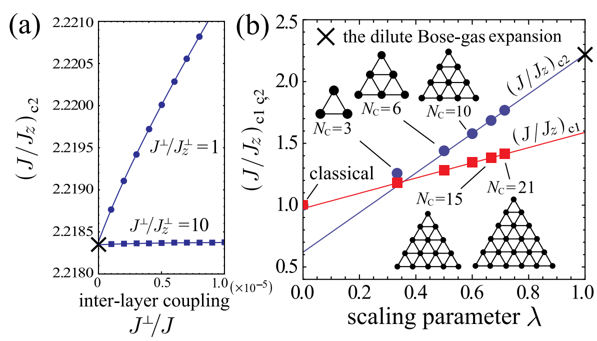

FIG. 3 (color online). (a) Coplanar-umbrella phase boundary $(J/J_z)_{c2}$ just below the saturation field as a function of the interlayer coupling strength obtained from $\Gamma_1 = \Gamma_2$. We display the cases of the isotropic (circles) and XY-type (squares) antiferromagnetic interlayer couplings as examples. (b) Cluster-size scaling of the CMF data for the phase boundaries $(J/J_z)_{c1}$ between 0- and π-coplanar phases as well as $(J/J_z)_{c2}$ just below the saturation field.

Degeneracy-lifting mechanism.—In Fig. 4(a), we plot the classical solution curve in the plane of the conjugate thermodynamic variables: J/J_z and the transverse nearest-neighbor correlation $\chi \equiv -\sum_{\langle i,j\rangle} \langle \hat{S}_i^x \hat{S}_j^x + \hat{S}_i^y \hat{S}_j^y \rangle / M$. At $J/J_z = 1$, there is a nontrivial continuous degeneracy of ground states in which the classical-spin vectors satisfy $\boldsymbol{S}_A + \boldsymbol{S}_B + \boldsymbol{S}_C = (0, 0, H/3J)$ with $|\boldsymbol{S}_\mu| = 1/2$ [17]. Figure 4(b) illustrates the peculiar mechanism of the quantum degeneracy lifting. The quantum fluctuations select the π-coplanar state out of the continuous manifold of the classical ground states. In the solution curve, the point of the π-coplanar state shown in Fig. 4(a) is extended to a finite section in Fig. 4(b). All of the other intermediate states form two separate sections of the solution curve with negative slope (negative "susceptibility"), which indicates the instability of those states. As a result, the classical ground-state degeneracy is broken up into two first-order transitions [see Fig. 4(c)].

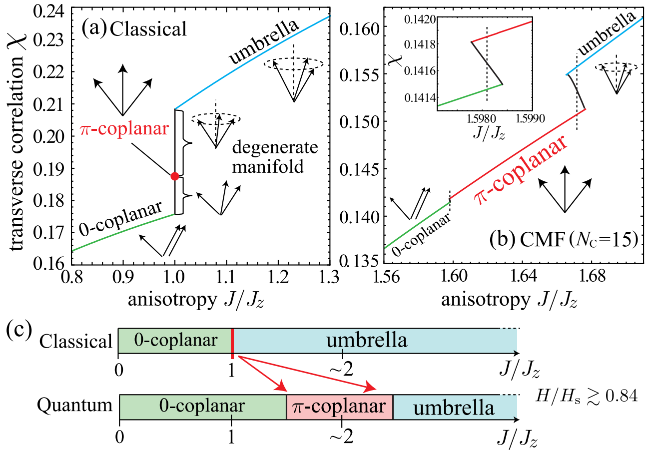

FIG. 4 (color online). (a) Classical solution of χ as a function of J/J_z for $H/J_z = 3$. (b) Quantum degeneracy lifting obtained by the CMF analysis ($H/J_z = 4.5$). The vertical dashed lines mark the first-order transition points determined by the Maxwell construction. The inset is the enlarged view around the weak first-order 0–π transition. The phase diagrams in (c) show the quantum breakup of the continuous degeneracy into two first-order transitions for $H/H_s \gtrsim 0.84$.

This novel degeneracy-lifting mechanism is sharply different from the known cases. For example, the square-lattice *XXZ* model also possesses a classical continuous degeneracy at the boundary of the spin-flop transition from the Néel to canted antiferromagnetic phase [57,58]. However, all of the intermediate states in the degenerate manifold are destabilized and only a single first-order transition is induced by the quantum effects [57–59] (see Ref. [49] for the direct comparison with Fig. 4). The same behavior also appears in certain bosonic systems such as spin-2 BECs at the transition boundaries to nematic phases [60]. In contrast, in the present model a specific intermediate state is chosen by quantum fluctuations from the degenerate manifold and occupies a finite region of the quantum phase diagram, whereas it does not appear in the classical one.

Remarks on experiments.—In the experiment of Ref. [23] on $Ba_3CoSb_2O_9$, the magnetization curve exhibits a cusp at $H \approx H_s/3$ for magnetic fields parallel to the c axis and a clear plateau is not detected. This can be understood within the phase diagram in Fig. 1(b) if the anisotropy is as large as $J/J_z \approx 1.3$. The authors in Ref. [23] have conjectured that a magnetization anomaly in $Ba_3CoSb_2O_9$ under transverse magnetic field $H \perp c$ may correspond to the 0–π transition of coplanar states, which is still controversial [24]. Moreover, the first-order 0–π transition for $H \| c$ is expected to be observed as a jump in the magnetization process by synthesizing a family material with larger easy-plane anisotropy $1.6 \lesssim J/J_z \lesssim 2.3$ or by tuning J/J_z with pressure [61] in spin-dimer compounds such as $Ba_3Mn_2O_8$ [40].

In the context of cold atomic or molecular systems, one could prepare the spin-$1/2$ *XXZ* system using, e.g., dipolar bosons with strong on-site repulsions in a triangular optical lattice [36–38]. The frustrated regime J, $J_z > 0$ could be accessed by the latest techniques, such as a fast oscillation of the lattice [31,33,34]. In the language of the hard-core boson, $1/2 - m_\mu^z$ and $[(m_\mu^x)^2 + (m_\mu^y)^2]^{1/2}$ correspond to the sublattice density filling and the sublattice BEC order parameter, respectively [62]. Therefore, the 0-coplanar state is regarded as a lattice supersolid (SS) state. Although the bosonic counterpart of the π-coplanar state also has the diagonal (density) and off-diagonal (BEC) orders simultaneously, it should be distinguished from the rigorous SS by the fact that the bosons on one of the three sublattices have no BEC order parameter. In other words, this state is partially disordered in the off-diagonal sector. Thus, the condensate flows on two sublattices avoiding the third, thus defining a honeycomb superlattice. We then refer to the π-coplanar state in the bosonic language as superlattice superfluid. Thus the 0–π transition of coplanar spin states is expected to be observed as a transition between the SS and superlattice-superfluid states in the optical-lattice quantum simulator. Since these two interesting phases exist for large easy-plane anisotropy, the required strength of the dipole-dipole interaction ($= J_z$) is relatively small compared to the hopping amplitude ($= |J|/2$), which is more advantageous than the conditions needed for the observation of the SS in the negative J/J_z side [36,45,46,55,56].

Conclusions.—We have studied the quantum phases of the spin-$1/2$ triangular-lattice *XXZ* model under magnetic fields motivated by the latest experimental developments in magnetism and optical-lattice systems. Using the dilute Bose-gas expansion and the CMF + S method, we established the entire quantum phase diagram including the frustrated regime and found that a nonclassical (π-)coplanar state emerges for strong fields. This is due to a particular lifting mechanism of the classical continuous degeneracy into two first-order transitions. We suggest that the quantum phase transition to the π-coplanar state can be observed in the magnetization process of triangular-lattice antiferromagnets with large easy-plane anisotropy or in the corresponding optical-lattice system.

The authors thank Tsutomu Momoi, Tetsuro Nikuni, Nikolay Prokof'ev, Hidekazu Tanaka, and Hiroshi Ueda for useful discussions. I. D. is supported by KAKENHI from JSPS Grants No. 25800228 and No. 25220711.

[1] G. Toulouse, Commun. Phys. **2**, 115 (1977).
[2] R. Moessner and A. R. Ramirez, Phys. Today **59**, No. 2, 24 (2006).
[3] L. Capriotti, A. E. Trumper, and S. Sorella, Phys. Rev. Lett. **82**, 3899 (1999).
[4] W. Zheng, J. O. Fjærestad, R. R. P. Singh, R. H. McKenzie, and R. Coldea, Phys. Rev. B **74**, 224420 (2006).
[5] S. R. White and A. L. Chernyshev, Phys. Rev. Lett. **99**, 127004 (2007).

[6] K. Harada, Phys. Rev. B **86**, 184421 (2012).
[7] A. V. Chubokov and D. I. Golosov, J. Phys. Condens. Matter **3**, 69 (1991).
[8] D. J. J. Farnell, R. Zinke, J. Schulenburg, and J. Richter, J. Phys. Condens. Matter **21**, 406002 (2009).
[9] T. Sakai and H. Nakano, Phys. Rev. B **83**, 100405(R) (2011).
[10] S Nishimoto, N Shibata, and C Hotta, Nat. Commun. **4**, 2287 (2013).
[11] L. Balents, Nature (London) **464**, 199 (2010).
[12] T.-H. Han, J. S. Helton, S. Chu, D. G. Nocera, J. A. Rodriguez-Rivera, C. Broholm, and Y. S. Lee, Nature (London) **492**, 406 (2012).
[13] F. Wang, F. Pollmann, and A. Vishwanath, Phys. Rev. Lett. **102**, 017203 (2009)
[14] H. C. Jiang, M. Q. Weng, Z. Y. Weng, D. N. Sheng, and L. Balents, Phys. Rev. B **79**, 020409(R) (2009).
[15] D. Heidarian and A. Paramekanti, Phys. Rev. Lett. **104**, 015301 (2010).
[16] M. Suzuki, *Quantum Monte Carlo Methods in Condensed Matter Physics* (World Scientific, Singapore, 1993).
[17] H. Kawamura and S. Miyashita, J. Phys. Soc. Jpn. **54**, 4530 (1985).
[18] S. Miyashita, J. Phys. Soc. Jpn. **55**, 3605 (1986).
[19] L. Seabra, T. Momoi, P. Sindzingre, and N. Shannon, Phys. Rev. B **84**, 214418 (2011).
[20] R. Chen, H. Ju, H.-C. Jiang, O. A. Starykh, and L. Balents, Phys. Rev. B **87**, 165123 (2013).
[21] Y. Shirata, H. Tanaka, A. Matsuo, and K. Kindo, Phys. Rev. Lett. **108**, 057205 (2012).
[22] H. D. Zhou, C. Xu, A. M. Hallas, H. J. Silverstein, C. R. Wiebe, I. Umegaki, J. Q. Yan, T. P. Murphy, J.-H. Park, Y. Qiu, J. R. D. Copley, J. S. Gardner, and Y. Takano, Phys. Rev. Lett. **109**, 267206 (2012).
[23] T. Susuki, N. Kurita, T. Tanaka, H. Nojiri, A. Matsuo, K. Kindo, and H. Tanaka, Phys. Rev. Lett. **110**, 267201 (2013).
[24] G. Koutroulakis, T. Zhou, C. D. Batista, Y. Kamiya, J. D. Thompson, S. E. Brown, and H. D. Zhou, arXiv:1308.6331.
[25] R. Coldea, D. A. Tennant, A. M. Tsvelik, and Z. Tylczynski, Phys. Rev. Lett. **86**, 1335 (2001).
[26] T. Ono, H. Tanaka, H. Aruga Katori, F. Ishikawa, H. Mitamura, and T. Goto, Phys. Rev. B **67**, 104431 (2003).
[27] N. A. Fortune, S. T. Hannahs, Y. Yoshida, T. E. Sherline, T. Ono, H. Tanaka, and Y. Takano, Phys. Rev. Lett. **102**, 257201 (2009).
[28] Y. Shimizu, K. Miyagawa, K. Kanoda, M. Maesato, and G. Saito, Phys. Rev. Lett. **91**, 107001 (2003).
[29] S. Trotzky, P. Cheinet, S. Fölling, M. Feld, U. Schnorrberger, A. M. Rey, A. Polkovnikov, E. A. Demler, M. D. Lukin, and I. Bloch, Science **319**, 295 (2008).
[30] J. Simon, W. S. Bakr, R. Ma, M. Eric Tai, P. M. Preiss, and M. Greiner, Nature (London) **472**, 307 (2011).
[31] J. Struck, C. Ölschläger, R. Le Targat, P. Soltan-Panahi, A. Eckardt, M. Lewenstein, P. Windpassinger, and K. Sengstock, Science **333**, 996 (2011).
[32] D. Greif, T. Uehlinger, G. Jotzu, L. Tarruell, and T. Esslinger, Science **340**, 1307 (2013).
[33] A. Eckardt, C. Weiss, and M. Holthaus, Phys. Rev. Lett. **95**, 260404 (2005).
[34] H. Lignier, C. Sias, D. Ciampini, Y. Singh, A. Zenesini, O. Morsch, and E. Arimondo, Phys. Rev. Lett. **99**, 220403 (2007).
[35] C. Becker, P. Soltan-Panahi, J. Kronjäger, S. Dörscher, K. Bongs, and K. Sengstock, New J. Phys. **12**, 065025 (2010).
[36] D. Yamamoto, I. Danshita, and C. A. R. Sá de Melo, Phys. Rev. A **85**, 021601(R) (2012).
[37] L. Pollet, J. D. Picon, H. P. Büchler, and M. Troyer, Phys. Rev. Lett. **104**, 125302 (2010).
[38] D. Yamamoto, T. Ozaki, C. A. R. Sá de Melo, and I. Danshita, Phys. Rev. A **88**, 033624 (2013).
[39] H. Nishimori and S. Miyashita, J. Phys. Soc. Jpn. **55**, 4448 (1986).
[40] E. C. Samulon, Y.-J. Jo, P. Sengupta, C. D. Batista, M. Jaime, L. Balicas, and I. R. Fisher, Phys. Rev. B **77**, 214441 (2008).
[41] A. B. Kuklov and B. V. Svistunov, Phys. Rev. Lett. **90**, 100401 (2003).
[42] E. Altman, W. Hofstetter, E. Demler, and M. D. Lukin, New J. Phys. **5**, 113 (2003).
[43] D. Yamamoto, A. Masaki, and I. Danshita, Phys. Rev. B **86**, 054516 (2012).
[44] T. Nikuni and H. Shiba, J. Phys. Soc. Jpn. **64**, 3471 (1995).
[45] S. Wessel and M. Troyer, Phys. Rev. Lett. **95**, 127205 (2005).
[46] L. Bonnes and S. Wessel, Phys. Rev. B **84**, 054510 (2011).
[47] G. Murthy, D. Arovas, and A. Auerbach, Phys. Rev. B **55**, 3104 (1997).
[48] E. G. Batuev and L. S. BraginskiSov. Phys. JETP **60**, 781 (1984).
[49] See Supplemental Material at http://link.aps.org/supplemental/10.1103/PhysRevLett.112.127203 for technical details and comparison with previous works.
[50] D. S. Fisher and P. C. Hohenberg, Phys. Rev. B **37**, 4936 (1988).
[51] G. Kotliar, S. Y. Savrasov, G. Pálsson, and G. Biroli, Phys. Rev. Lett. **87**, 186401 (2001).
[52] P. Anders, E. Gull, L. Pollet, M. Troyer, and P. Werner, Phys. Rev. Lett. **105**, 096402 (2010).
[53] D.-S. Lühmann, Phys. Rev. A **87**, 043619 (2013).
[54] The first-order nature of the transition between the uniform (superfluid) and three-sublattice (supersolid) states for $H \neq 0$ is overlooked in Ref. [45]. See Refs. [36,46,55].
[55] X.-F. Zhang, R. Dillenschneider, Y. Yu, and S. Eggert, Phys. Rev. B **84**, 174515 (2011).
[56] M. Boninsegni and N. Prokof'ev, Phys. Rev. Lett. **95**, 237204 (2005); D. Heidarian and K. Damle, *ibid.* **95**, 127206 (2005); R. G. Melko, A. Paramekanti, A. A. Burkov, A. Vishwanath, D. N. Sheng, and L. Balents, *ibid.* **95**, 127207 (2005); A. Sen, P. Dutt, K. Damle, and R. Moessner, *ibid.* **100**, 147204 (2008).
[57] M. Holtschneider, S. Wessel, and W. Selke, Phys. Rev. B **75**, 224417 (2007).
[58] M. Kohno and M. Takahashi, Phys. Rev. B **56**, 3212 (1997).
[59] G. G. Batrouni and R. T. Scalettar, Phys. Rev. Lett. **84**, 1599 (2000).
[60] N. T. Phuc, Y. Kawaguchi, and M. Ueda, Phys. Rev. A **88**, 043629 (2013).
[61] Ch. Rüegg, B. Normand, M. Matsumoto, A. Furrer, D. F. McMorrow, K. W. Krämer, H.-U. Güdel, S. N. Gvasaliya, H. Mutka, and M. Boehm, Phys. Rev. Lett. **100**, 205701 (2008).
[62] H. Matsuda and T. Tsuneto, Suppl. Prog. Theor. Phys. **46**, 411 (1970).